



ELSEVIER

2 November 2000

Physics Letters B 492 (2000) 245–253

PHYSICS LETTERS B

www.elsevier.nl/locate/npe

Superdeformation in ^{91}Tc

E. Ideguchi ^{a,*}, B. Cederwall ^a, R. Wyss ^a, T. Bäck ^a, K. Lagergren ^a, A. Johnson ^a,
W. Klamra ^a, J. Cederkäll ^{a,1}, M. Devlin ^{b,2}, J. Elson ^b, D.R. LaFosse ^{b,3}, F. Lerma ^{b,4},
D.G. Sarantites ^b, V. Tomov ^b, M. Hausmann ^c, A. Jungclaus ^c, D.R. Napoli ^d,
M.P. Carpenter ^e, R.V.F. Janssens ^e, F.G. Kondev ^e, T. Lauritsen ^e, C.J. Lister ^e,
D. Seweryniak ^e, I. Wiedenhoever ^e, R.M. Clark ^f, P. Fallon ^f, I.Y. Lee ^f,
A.O. Macchiavelli ^f, R.W. Macleod ^{f,5}

^a Department of Physics, Royal Institute of Technology, Frescativägen 24, S-104 05 Stockholm, Sweden

^b Chemistry Department, Washington University, St. Louis, MI 63130, USA

^c II. Physikalisches Institut, University of Göttingen, Göttingen, Germany

^d Laboratori Nazionali di Legnaro, INFN, Italy

^e Argonne National Laboratory, 9700 S. Cass Avenue, Argonne, IL 60439, USA

^f Nuclear Science Division, Lawrence Berkeley Laboratory, Berkeley, CA 94720, USA

Received 23 May 2000; received in revised form 31 August 2000; accepted 14 September 2000

Editor: V. Metag

Abstract

A high-spin rotational band with 11 γ -ray transitions has been observed in ^{91}Tc . The dynamical moment of inertia as well as the transition quadrupole moment of $8.1_{-1.4}^{+1.9} \text{ eb}$ measured for this band show the characteristics of a superdeformed band. However, the shape is more elongated than in the neighbouring $A = 80\text{--}90$ superdeformed nuclei. Theoretical interpretations of the band within the cranked Strutinsky approach based on two different Woods–Saxon potential parameterisations are presented. Even though an unambiguous configuration assignment proved difficult, both calculations indicate a larger deformation and at least three additional high- N intruder orbitals occupied compared to the lighter SD nuclei. © 2000 Elsevier Science B.V. All rights reserved.

PACS: 21.10.Re; 21.60.Cs; 23.20.Lv; 27.50.+e

* Corresponding author.

E-mail address: ideguchi@msi.se (E. Ideguchi).

¹ Current address: CERN, EP, CH-1211, Geneva 23, Switzerland.

² Current address: LANSCE-3, LANL, Los Alamos, NM 87545, USA.

³ Current address: Dept. of Physics and Astronomy, SUNY-Stony Brook, NY 11794, USA.

⁴ Current address: Dept of Radiation Oncology, Washington University, St. Louis, MO 63130, USA.

⁵ Current address: Physics Division, TJNAF, Newport News, VA 23606, USA.

Since the initial discovery of a superdeformed (SD) rotational band in ^{152}Dy [1], a multitude of SD bands have been identified in the mass regions, $A \sim 130, 150, 190$ [2]. In addition nuclei ascribed to have triaxial superdeformed shapes have been reported around mass 165 [3]. These bands were studied with the aid of large high-purity Ge detector arrays [4,5]. The increased sensitivity obtained by combining the latest generation of γ -ray spectrometers with charged particle detectors has made it possible to identify other regions of superdeformation. Several SD bands have been found in the mass 80 region [6,7] and, more recently, around mass 60 [8] and mass 70 [9]. These experimental results have confirmed earlier theoretical predictions [10–13]. In a recent investigation of $A \approx 90$ nuclei, superdeformed bands were identified in ^{88}Mo [14] and ^{89}Tc [15]. The SD states of these nuclei were reported to have large quadrupole deformations with deformation parameters $\beta_2 \approx 0.6$. These findings were in agreement with Cranked Woods–Saxon–Strutinsky calculations, which predicted $Z = 42$ and $Z = 43$ to be favoured particle numbers at SD shapes in $A \approx 90$ nuclei [14,15].

Both the calculations and the experimental findings indicate that the SD mass 80 and 90 regions are different in character. In the $A \approx 90$ ($46 \leq N \leq 54$) region, the low-lying states are mainly based on particle–hole excitations at a near spherical shape. In contrast, the low-lying yrast states of nuclei in the mass 80 ($N \leq 44$) region exhibit collectivity with rotational-like band structures of enhanced E2 transitions (see [13] and references therein). Therefore, the new $A \approx 90$ SD region resembles the $A \sim 150$ and $A \sim 190$ SD regions, with large differences in structure and shape between SD and low-lying yrast states. In this paper we report on the observation of a SD band in ^{91}Tc obtained as a result of a systematic investigation of SD shapes in $A \approx 90$ nuclei.

High-spin states in ^{91}Tc were studied using the $^{58}\text{Ni}(^{40}\text{Ca}, \alpha 3\text{p})^{91}\text{Tc}$ reaction in two separate experiments. In the first one, a ^{40}Ca beam of 185 MeV was provided by the 88-inch Cyclotron of the Lawrence Berkeley National Laboratory. A self-supporting 0.38 mg/cm^2 enriched ^{58}Ni target was used. It was placed at an angle of 30° relative to the beam direction, resulting in an effective thickness of 0.44 mg/cm^2 . The GAMMASPHERE array [5] comprising 94

escape-suppressed germanium detectors and the Microball [17], a 4π array of 95 CsI(Tl) scintillation counters, were used to detect γ -rays and charged particles, respectively, emitted in the reactions. The charged particles were identified by using pulse shape discrimination on the signals from the CsI(Tl) scintillators. With a trigger condition of three or more escape-suppressed Ge detectors firing in coincidence, a total of 2.4×10^9 events were collected on magnetic tapes.

In the second experiment, a 185 MeV ^{40}Ca beam provided by the ATLAS linear accelerator at the Argonne National Laboratory was used to bombard a self-supporting enriched ^{58}Ni target of 0.41 mg/cm^2 thickness. A beam charge state of 19^+ was used in order to avoid the possible contamination of Ar ions in the beam. The detector setup consisted of the GAMMASPHERE array comprising 88 escape-suppressed Ge detectors, the 95-element CsI(Tl) Microball array, 20 neutron detectors, and the FMA recoil separator [18]. The neutron detectors were placed in the forward rings of the GAMMASPHERE array at angles between 17 and 50 degrees relative to the beam direction. The heavymet collimators were removed from the BGO shields in GAMMASPHERE so that γ -ray multiplicity and sum-energy information from both Ge and BGO detectors could be obtained. A composite trigger condition for the data acquisition system was set up in order to collect either at least one neutron together with at least two γ rays or three- and higher-fold γ -coincidence events. A total of 8.7×10^8 events were stored on magnetic tapes. By using the information from the particle detectors, events were sorted off-line into a symmetrised E_γ – E_γ correlation matrix for each evaporation channel. However, the direct channel selection is limited by the efficiency of the particle detector system and by the occasional misinterpretation of charged particle signals. The 1-alpha 3-proton gated $\gamma\gamma$ matrix therefore contains contaminations from other evaporation channels, i.e. $1\alpha 4\text{p}$ (^{90}Mo), $1\alpha 5\text{p}$ (^{89}Nb), $2\alpha 3\text{p}$ (^{87}Nb) and $2\alpha 2\text{p}$ (^{88}Mo), where the contamination from the $2\alpha 2\text{p}$ channel was caused by mis-identification of low-energy α particles as protons. The contribution from other contaminating reaction channels are negligibly small due to their low cross sections. A “cleaned” $\gamma\gamma$ correlation matrix due to ^{91}Tc was produced by subtracting matrices

from the contaminating channels with appropriate normalisation factors.

The high-spin level structure of ^{91}Tc has previously been studied [19] up to the 12.2 MeV level. Both positive and negative parity states were assigned up to $47/2^+$ at 10.505 MeV and $(45/2^-)$ at 9.717 MeV, respectively.

In the spectral region from 1350 keV to 2424 keV, the present work has revealed a new rotational cascade with 11 transitions. Fig. 1 shows the γ -ray spectrum obtained by summing double coincidence gates set on

the members of this band in the three- and higher-fold data. The γ -ray peaks belonging to the band are labelled by their energies and uncertainties in keV. The band is in coincidence with known γ -ray transitions in ^{91}Tc [19]. Symbols below 1.3 MeV indicate the peaks of the previously reported γ rays from positive (open circles) and negative (crosses) parity states in ^{91}Tc , respectively. In the spectrum gated by the band no γ rays originating from other evaporation channels were observed. This assigns the new band unambiguously to ^{91}Tc .

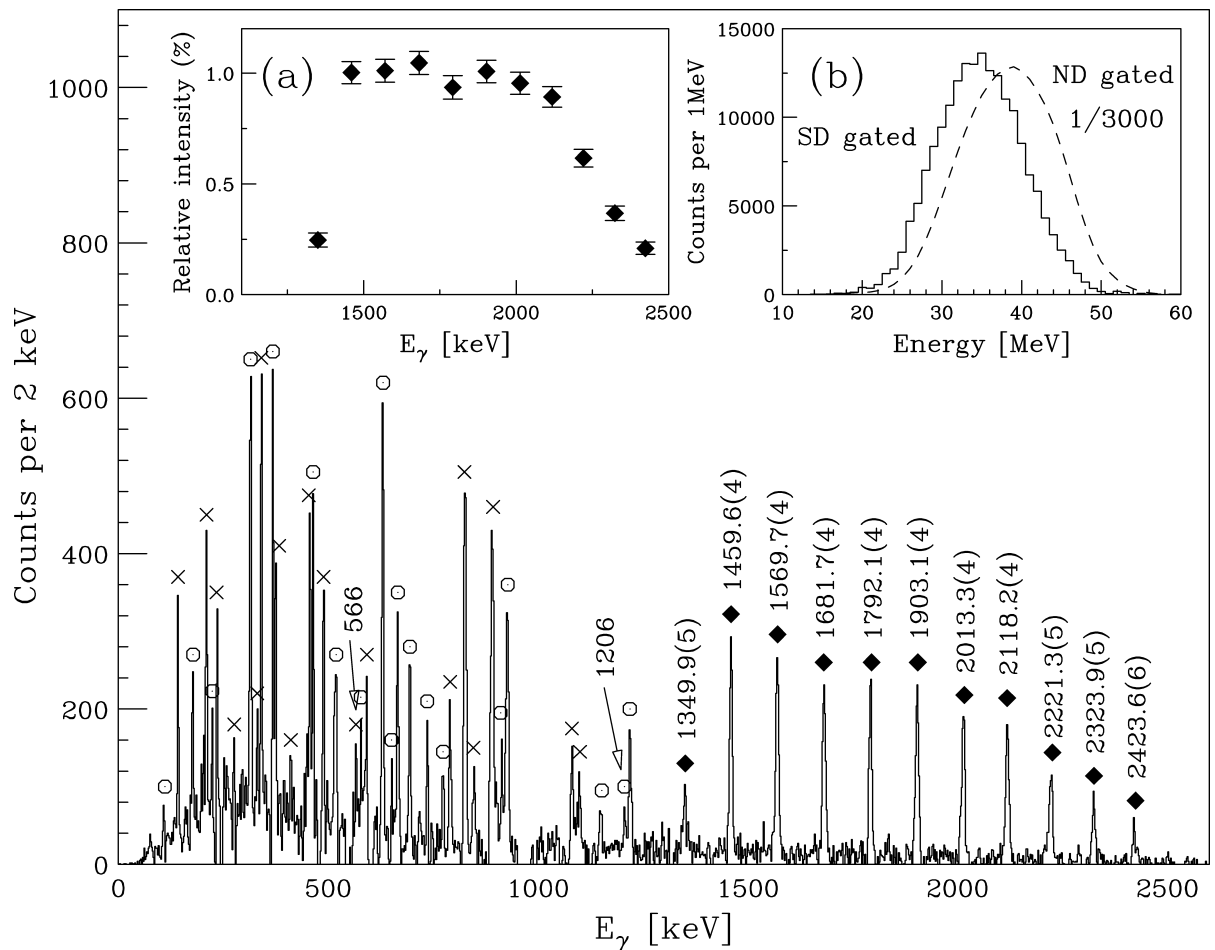


Fig. 1. Coincidence γ -ray spectrum obtained by double gating on all transitions of the new band (filled diamonds) in the $1\alpha 3p$ -gated data. Previously reported transitions between low-lying positive (open circles) and negative (crosses) parity states appear in coincidence with the band. The 566 and 1206 keV transitions depopulate states with $I^\pi = 47/2^+$ at 10.505 MeV and $(41/2^-)$ at 8.559 MeV, respectively. Inset (a) shows the relative intensity profile of the new band. The summed energy spectra of charged particles obtained by double γ gating on the low-lying transitions (dashed line) and the new band (solid line) are shown in inset (b).

The relative intensities of the in-band transitions are shown in of Fig. 1(a). The general feature of this intensity distribution is characteristic of SD nuclei. The intensity gradually increases as the γ -ray energy decreases, flattens out at the maximum, and then drops rapidly as the band decays to the low-lying states. The plateau region corresponds to $\sim 1\%$ of the channel intensity.

In the present study, the linking transitions between the band and known low-lying states were not observed. However, the high-spin nature of the band is revealed by its decay into known high-spin states. The 1206 keV and 566 keV transitions observed in coincidence with the band originate from states with $I^\pi = 47/2^+$ at 10.505 MeV and $(41/2^-)$ at 8.559 MeV, respectively.

Fig. 1(b) shows histograms of the sum of the particle kinetic energies, T_p , in the centre of mass frame, obtained by setting double γ gates on the transitions of the new band (solid line) and transitions between low-lying states (dashed line), respectively. The mean T_p value of 34.0 MeV for events gated by the band is 4 MeV below the average measured in coincidence with low-lying transitions. This indicates that the band is populated by the components with the highest excitation energy and the highest spin in the ^{91}Tc entry distribution.

Fig. 2(a) compares the dynamical moments of inertia, $J^{(2)}$, for the new band with those of ^{88}Mo [14] and ^{89}Tc [15] as a function of rotational frequency. The $J^{(2)}$ values of ^{91}Tc are almost constant at around $36 \hbar^2/\text{MeV}$ up to 1.0 MeV of rotational frequency, and increase above this frequency. On the other hand, the $J^{(2)}$ values of ^{88}Mo and ^{89}Tc show a gradual decrease down to $25 \hbar^2/\text{MeV}$ around 1.0 MeV. The significantly larger $J^{(2)}$ values for the band in ^{91}Tc may suggest a larger deformation than in the neighbouring SD nuclei, ^{88}Mo and ^{89}Tc , which were reported to have quadrupole deformations of $\beta_2 \approx 0.6$.

The $J^{(2)}$ -moments of inertia of ^{91}Tc were also compared with those of typical SD bands in other mass regions in Fig. 2(b). In order to remove the mass dependence, a scaling factor of $1/A^{5/3}$ [20] was applied. The scaled $J^{(2)}$ values of ^{91}Tc are comparable with or even larger than those of ^{152}Dy and significantly larger than those in the mass 80 and 60 regions. One exception is the case of ^{86}Zr [21], where a SD band has been observed with a $J^{(2)}$ -moment of inertia of simi-

lar magnitude to that observed in ^{91}Tc . However, in the ^{86}Zr case the large moment of inertia was not attributed to enhanced deformation. Instead, a possible “multiple band crossing” scenario was suggested. The experimental Q_t value of the ^{86}Zr band was reported to be $5.4_{-1.2}^{+2.2} \text{eb}$ [21].

The observed large $J^{(2)}$ -moment of inertia for the new band of ^{91}Tc accentuates the need to measure the transition quadrupole moment, Q_t , as a mean to assess its deformation. This was achieved by using a residual Doppler shift method [14,22]. In Fig. 3 the fractional Doppler shift values, $F(\tau)$, are plotted as a function of the γ -ray energy. Data points for low-lying (filled circles) and SD (open squares) transitions, respectively, are extracted from the residual Doppler shifts of the γ -ray energies measured in the forward and backward detectors. The deduced $F(\tau)$ values were compared with calculated values based on the known stopping powers [23]. In the calculation a side-feeding cascade of two transitions into each state was assumed. These side-feeding cascades are furthermore assumed to have the same Q_t and moment of inertia as the band in question. The SD data are best fitted with $Q_t = 8.1_{-1.4}^{+1.9} \text{eb}$. The quoted uncertainties do not include systematic errors arising e.g. from those in the stopping powers. The deduced Q_t value corresponds to a quadrupole deformation of $\beta_2 \approx 0.69$, assuming an axially symmetric prolate shape, and using the expression for Q_t given in Ref. [24].

The deduced Q_t value of the SD band in ^{91}Tc is compared with those measured in other mass regions [25] in Fig. 4. In order to remove the A and Z dependences of the quadrupole moments, they were divided by Z and R^2 , where $R = r_0 A^{1/3}$ and $r_0 = 1.2 \text{ fm}$. The result supports the SD character of this band and indicates a large deformation, comparable to those in the SD $A \sim 150$ region and in the fission isomer region. The deduced Q_t value is consistent with the large $J^{(2)}$ -moment of inertia of the band shown in Fig. 2(b).

The pronounced difference between the moments of inertia of the SD bands in ^{91}Tc and in ^{89}Tc [15] implies that the addition of two neutrons has a dramatic effect on the structure of the SD bands. In order to investigate this theoretically, cranked Strutinsky calculations based on a Woods–Saxon (WS) potential [26] were performed. Pairing correlations were taken into account by means of a seniority and dou-

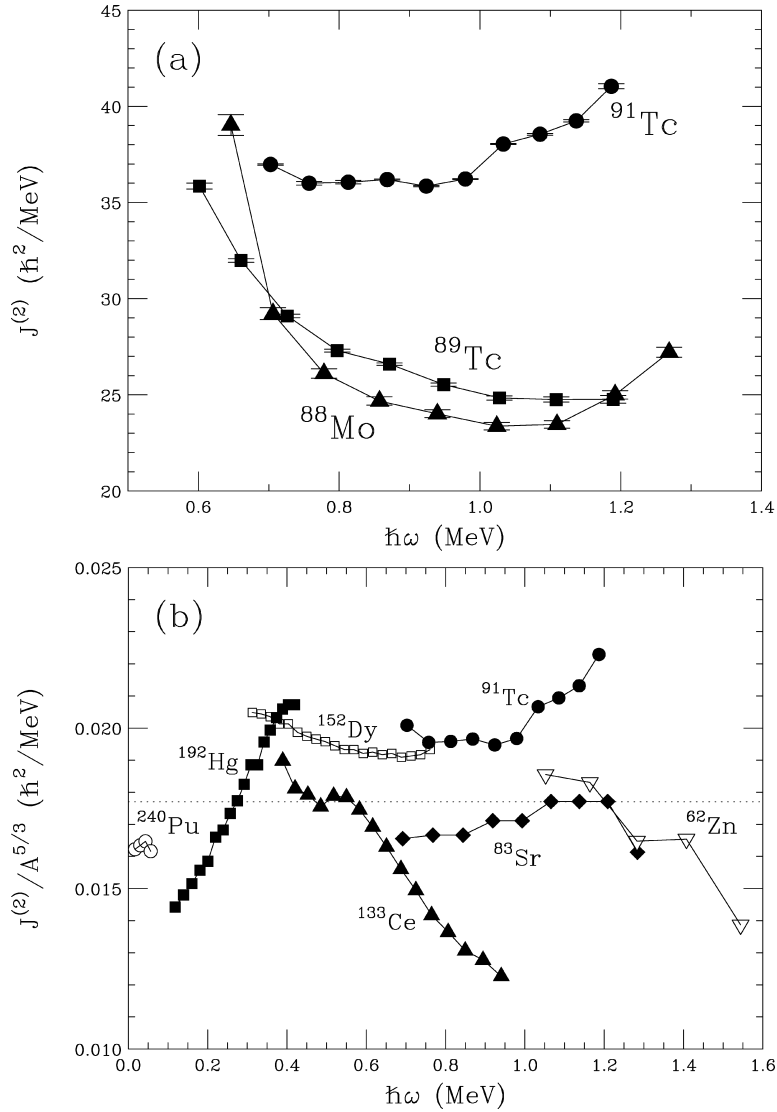


Fig. 2. Plots of dynamical moments of inertia, $J^{(2)}$, versus rotational frequency. (a) $J^{(2)}$ values for the new band in ^{91}Tc and for the SD bands in ^{88}Mo and ^{89}Tc . (b) The scaled moments of inertia $J^{(2)}/A^{5/3}$, for the SD bands in ^{240}Pu , ^{192}Hg , ^{152}Dy , ^{133}Ce , ^{83}Sr , ^{62}Zn [8,25] and the new band in ^{91}Tc . The dotted line represents the moment of inertia of a rigid rotor with quadrupole deformation $\beta_2 = 0.5$.

ble stretched quadrupole pairing force [27]. Approximate particle number projection was performed via the Lipkin–Nogami method [28,29]. Each quasiparticle configuration was blocked self-consistently. The energy in the rotating frame of reference was minimised with respect to the deformation parameters β_2 , β_4 and γ .

For both ^{89}Tc and ^{91}Tc , the most favoured SD configurations were calculated to be based on a single $h_{11/2}$ proton and two $h_{11/2}$ neutrons, due to the presence of a large shell gap at $Z = 43$ [14,15]. This configuration is similar to those of the other SD bands in this mass region [16]. Adopting the convention of Ref. [30], it is denoted as $\pi 5^1 \nu 5^2$, reflecting the

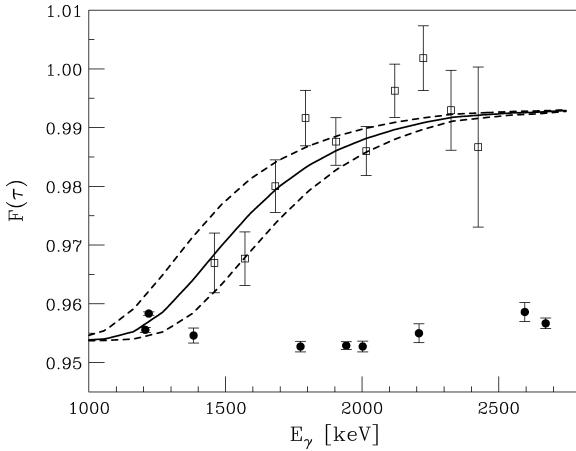


Fig. 3. Fractional Doppler shift $F(\tau)$ as a function of γ -ray energy. Data points for low-lying transitions (filled circles) and SD band transitions (open squares) are extracted from the residual Doppler shifts of the γ -ray energies in the forward and backward detectors. The solid line represents $Q_t = 8.1 \text{ eb}$, and the dashed lines correspond to the quoted uncertainties.

number of particles occupying high- N orbits. The moments of inertia of these two bands are calculated to be quite similar. However, whereas the calculated and experimentally deduced moments of inertia agree rather well for ^{89}Tc [15], they certainly do not for the case of ^{91}Tc . The observed SD band in ^{91}Tc can not be assigned to the $\pi 5^1\nu 5^2$ configuration which is predicted to be energetically most favoured. To check the sensitivity of these results to the details of the WS potential, calculations were performed with different potential parameterisations.

The predicted energies of favoured spherical and SD configurations for ^{89}Tc and ^{91}Tc are shown as a function of spin in Fig. 5. We may note that the SD band observed for ^{89}Tc is among the most intense SD bands known, with an intensity ratio of SD to normal deformed (ND) states of approximately 15% [15]. The calculations are in fair agreement with the observed low-lying states, and show that in the low-spin regime, the yrast SD states of ^{91}Tc are about 3 MeV higher in energy than those of ^{89}Tc , with respect to the spherical states. For both nuclei, the

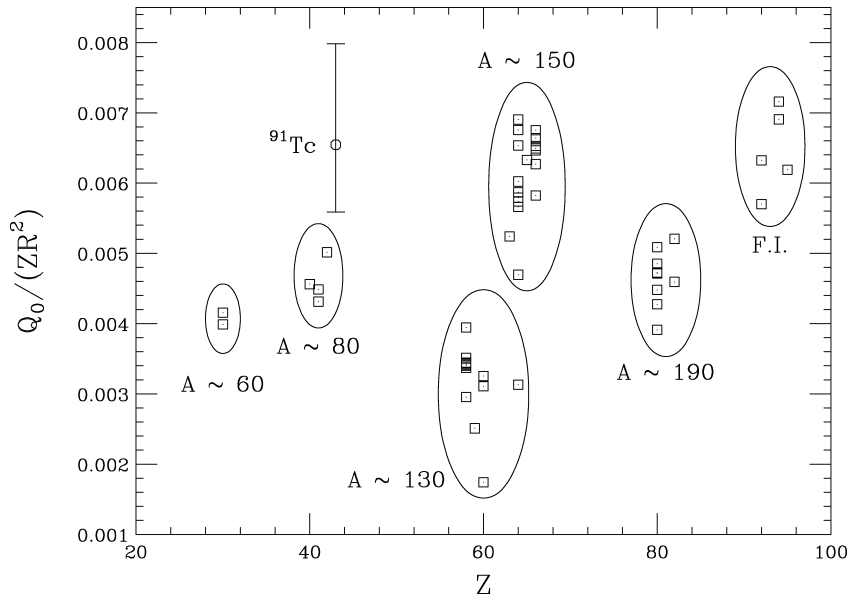


Fig. 4. Scaled quadrupole moments for SD bands in the mass 60, 80, 130, 150 and 190 regions and those of the fission isomer region. Q_0 indicates transition or intrinsic quadrupole moments from lifetime (DSAM or RDM) data [25]. In order to remove the A and Z dependences of the quadrupole moments, they were divided by Z and R^2 ($R = r_0 A^{1/3}$).

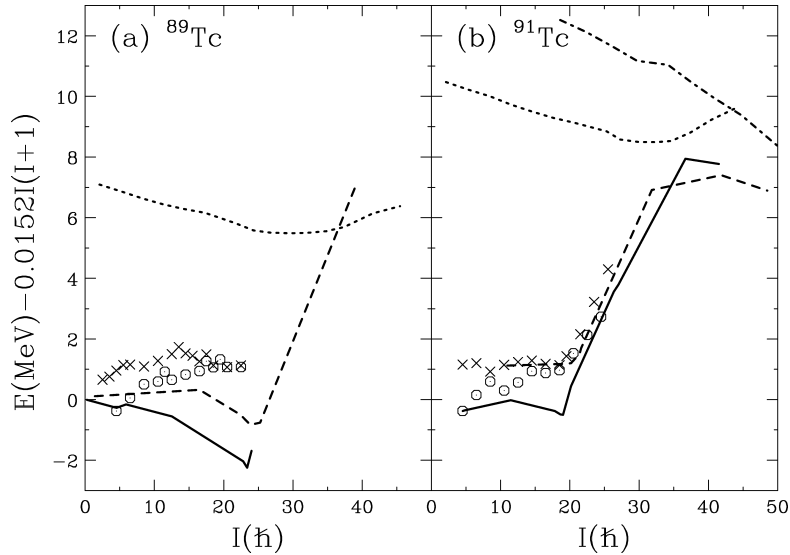


Fig. 5. Energy as a function of spin for the calculated spherical and SD configurations in ^{89}Tc (a) and ^{91}Tc (b). The WS parameterisation of Refs. [14–16] was used for these plots. Dotted and dot-dashed lines correspond to favoured SD configurations, $\pi 5^1\nu 5^2$ and $\pi 5^2\nu 5^3(6^1)$, respectively. Solid and dashed lines indicate spherical positive parity and spherical negative parity states, respectively. The experimentally observed low-lying positive parity (open circles) and negative parity (crosses) states are also plotted.

available spin within the $N = 3$ shell is limited, having a maximum of $49/2\hbar$ for ^{91}Tc and $57/2\hbar$ for ^{89}Tc . In ^{91}Tc , particle–hole (ph) excitations across the $N = 50$ gap can compete with the SD states as opposed to the situation in ^{89}Tc . For the case of ^{91}Tc , even the spherical states involving the $2p-2h$ excitation into the $d_{5/2}-g_{7/2}$ shell as well as $h_{11/2}$ occupation, having a maximum spin of $I = 73/2\hbar$, are lower in energy than the corresponding SD states. Additional ph excitations also compete favourably with the SD structures. Consequently, none of the SD configurations in ^{91}Tc become yrast in the calculated spin range as can be seen in Fig. 5.

In contrast, the calculated SD configuration of ^{89}Tc becomes yrast around $I \approx 37\hbar$. This is in reasonable agreement with the observed depopulation of the SD band [15], where the highest spin value was estimated to be $79/2\hbar$. In ^{91}Tc the highest spin of low-lying states populated in coincidence with the SD band is $47/2\hbar$. By assuming an average spin cost of $2\hbar$ to connect the lowest SD state with the $47/2\hbar$ state, the highest spin of the SD band can be estimated to be $95/2\hbar$.

The predicted scenario for ^{91}Tc shown in Fig. 5, may not easily be reconciled with the observation of SD states at all. However, the calculations may qualitatively lend an interpretation to the observed SD structure. Above $I = 43\hbar$ a more deformed (“enhanced”) SD configuration built on a larger number of occupied high- N intruder orbits crosses the $\pi 5^1\nu 5^2$ SD configuration. The more deformed SD configuration has properties which are in better agreement with the experimental $J^{(2)}$ -moment of inertia, as discussed below. This might indicate that the ^{91}Tc SD band is fed at spins above $I = 43\hbar$, which in fact is in rough agreement with the observed depopulation of the band. In the spin $I \geq 40\hbar$ region, the SD configuration corresponding to the dot-dashed line in Fig. 5 is one out of several configurations close to the Fermi surface. There is no pronounced shell structure and which configuration is lowest in energy depends sensitively on the details of the potential parameters. Therefore, it is difficult to unambiguously assign a particular quasi-particle configuration to the newly discovered band. Below, results based on two different parameterisations of the WS potential are shown.

For the WS potential parameterisation employed in recent studies of this mass region [14–16], the lowest SD structure at $I \geq 43 \hbar$ corresponds to a hole state in the proton $g_{9/2}$ orbit, two protons being promoted into the $N = 5$ orbits. For the neutrons, three $N = 5$ orbits are occupied. Compared to the SD band in ^{89}Tc , two more $N = 5$ orbitals are predicted to be occupied and the quadrupole moment is calculated to be $Q_0 \approx 6.5 \text{ eb}$, i.e. 1 eb larger than in ^{89}Tc . The minimum starts out at axial symmetry ($\beta_2 = 0.57$), but becomes very soft with increasing spin. At $\hbar\omega \approx 1.2 \text{ MeV}$ the shape becomes triaxial ($\gamma \approx 15^\circ$) induced by the occupation of the $N = 6$ intruder orbital. In this scenario the rise of the $J^{(2)}$ -moment of inertia, starting at $\hbar\omega \approx 1.0 \text{ MeV}$ (Fig. 6(a)), is caused by the occupation of the $N = 6$ orbital, which polarises the nucleus towards slightly larger β_2 and positive γ values.

For the Chepurnov parameterisation of the WS potential, previously used in a study of SD shapes in the $A \sim 190$ region [31], the lowest configuration in the regime of $I > 40 \hbar$ also has negative parity, arising from the proton orbitals in this case. Here, two $h_{11/2}$ protons are calculated to be occupied and a hole state

is present in the strongly up-sloping $f_{7/2}$, $\Omega = 7/2$ orbit. Such a structure would in principle give rise to a pair of strongly coupled signature partner bands. However, in the high angular momentum regime, the two signatures are split due to mixing with other orbitals and, perhaps, only one of the signature partner bands is populated with sufficient intensity to be observed. The calculated moment of inertia is in reasonable agreement with our data, see Fig. 6(b). The deformation of this structure is calculated to be $\beta_2 \approx 0.7$, corresponding to a $Q_0 \approx 9 \text{ eb}$. This would imply the largest deformation of a SD band discovered so far. The large hump in the calculated moment of inertia at $\hbar\omega \approx 1.2 \text{ MeV}$ is caused by a similar occupation of the $N = 6$ orbital as for the other potential. Due to a weaker spin–orbit coupling in the Chepurnov parameterisation, this band crossing occurs at a larger rotational frequency, although the deformation is considerably larger. In terms of high- N intruder orbits, one can classify this structure as a $\pi 5^2 \nu 5^4$ configuration, below the $N = 6$ band crossing.

In both potential parameter sets, the $N = 6$ orbital is close to the Fermi surface at the highest

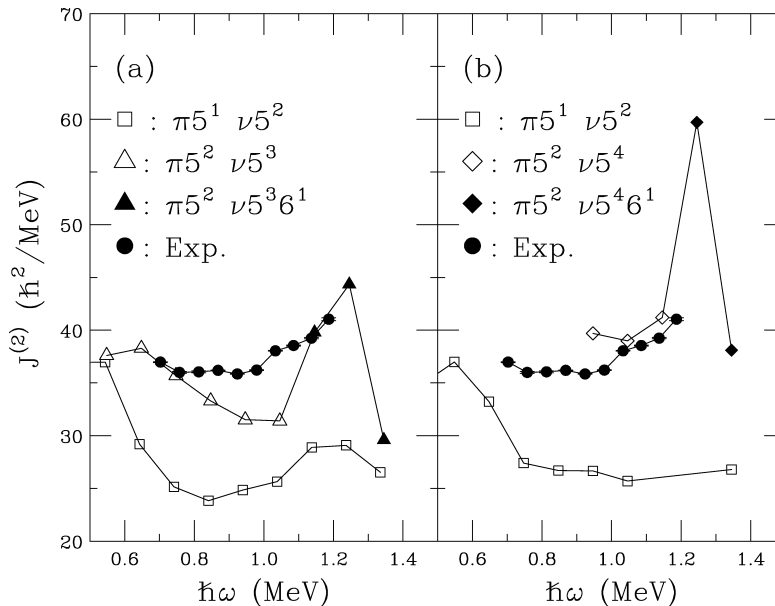


Fig. 6. Calculated $J^{(2)}$ -moments of inertia with two different parameterisations of the Woods–Saxon potential, (a) [14–16], (b) [31], and experimentally deduced $J^{(2)}$ values.

observed angular momenta. Since it lies two major shells above the spherical states, it is an important probe of the spin–orbit interaction in atomic nuclei.

A general feature of the calculations is the competition between SD and “enhanced” SD configurations. The latter have larger deformation and larger occupation of high- N intruder orbitals. Although we may not assign the observed SD band to a specific quasiparticle configuration in the present work, the calculations suggest that a band based on this latter type of configuration is here observed experimentally for the first time.

In summary, a discrete-line superdeformed band has been identified in ^{91}Tc , consisting of eleven transitions. The scaled $J^{(2)}$ -moment of inertia for this band is comparable to those of SD bands in the $A \sim 150$ mass region and considerably larger than those previously observed in the $A \sim 80$ SD region. The large value of the experimentally deduced transition quadrupole moment ($Q_t = 8.1_{-1.4}^{+1.9} \text{ eb}$) provides further evidence for enhanced superdeformation relative to the SD bands observed in the lighter neighbours. The detailed structure of the SD band is difficult to assign unambiguously. Similar to studies of nuclei far from stability, the very high-spin states in ^{91}Tc are probing a regime of single particle levels inaccessible previously, where theoretical assignments are associated with large uncertainties. Two different scenarios, built upon different intruder contents, were presented. In both scenarios the calculated deformation is larger and at least three additional high- N orbitals are occupied than in the SD band in ^{89}Tc . Accurate lifetime measurements may help to further distinguish between different interpretations.

Acknowledgements

The authors wish to thank the operating crews of the LBNL 88-inch Cyclotron and the ANL ATLAS linear accelerator for their assistance in the experiments. We would like to thank John Greene for preparing targets. This work was supported by the Swedish Natural Science Research Council, The Göran Gustafsson

foundation, The Scandinavia–Japan Sasakawa foundation (grant No. NS98-2) and the US Department of Energy, grant No. DE-FG05-88ER40406 (Washington University) and contracts Nos. DE-AC03-76SF00098 (LBNL) and W-31-109-ENG-38 (ANL).

References

- [1] P.J. Twin et al., Phys. Rev. Lett. 57 (1986) 811.
- [2] X.-L. Han, C.-L. Wu, At. Data Nucl. Data Tables 63 (1996) 117.
- [3] W. Schmitz et al., Phys. Lett. B 303 (1993) 230; S. Törmänen et al., Phys. Lett. B 454 (1999) 8, and references therein.
- [4] J. Simpson, Z. Phys. A 358 (1997) 139.
- [5] I.Y. Lee, Nucl. Phys. A 520 (1990) 641c.
- [6] C. Baktash et al., Phys. Rev. Lett. 74 (1994) 1946.
- [7] D.R. LaFosse et al., Phys. Rev. Lett. 78 (1997) 614.
- [8] C.E. Svensson et al., Phys. Rev. Lett. 79 (1997) 1233.
- [9] M. Devlin et al., Phys. Rev. Lett. 82 (1999) 5217.
- [10] I. Ragnarsson, in: Proc. Workshop on The Science of Intense Radioactive Ion Beams, Los Alamos, 1990, p. 199.
- [11] J. Dudek, W. Nazarewicz, N. Rowley, Phys. Rev. C 35 (1987) 1489.
- [12] R. Wyss, Slide report, in: Euroball Collaboration Meeting, Strasbourg, 1994.
- [13] A.V. Afanasjev, I. Ragnarsson, Nucl. Phys. A 586 (1995) 377.
- [14] T. Bäck et al., Eur. Phys. J. A 6 (1999) 391.
- [15] B. Cederwall et al., Eur. Phys. J. A 6 (1999) 251.
- [16] F. Lerma et al., Phys. Rev. Lett. 83 (1999) 5447.
- [17] D.G. Sarantites et al., Nucl. Instrum. Meth. A 381 (1996) 418.
- [18] Cary N. Davids, J.D. Larson, Nucl. Instrum. Meth. B 40/41 (1989) 1224.
- [19] D. Rudolph et al., Phys. Rev. C 49 (1994) 66.
- [20] D.F. Winchell et al., Phys. Lett. B 289 (1992) 267.
- [21] D.G. Sarantites et al., Phys. Rev. C 57 (1998) R1.
- [22] B. Cederwall et al., Nucl. Instrum. Meth. A 354 (1995) 591.
- [23] J.F. Ziegler, J.P. Biersack, U. Littmark, The Stopping and Ranges of Ions in Matter, Vol. 1, Pergamon, London, 1985.
- [24] W. Nazarewicz, R. Wyss, A. Johnson, Nucl. Phys. A 503 (1989) 285.
- [25] Balraj Singh, Richard B. Firestone, S.Y. Frank Chu, Table of superdeformed nuclear bands and fission isomers, LBL-38004, (1997) and references therein.
- [26] S. Ćwiok et al., Comp. Phys. Commun. 46 (1987) 379.
- [27] W. Satuła, R. Wyss, Phys. Scr. T 56 (1995) 159.
- [28] W. Satuła, R. Wyss, P. Magierski, Nucl. Phys. A 578 (1994) 45.
- [29] Y. Nogami, H.C. Pradhan, J. Law, Nucl. Phys. A 201 (1973) 357.
- [30] T. Bengtsson et al., Phys. Lett. B 208 (1988) 39.
- [31] W. Satuła, R. Wyss, Phys. Rev. C 50 (1994) 2888.